# COMPARISON OF MEASURED AND COMPUTED BSDF OF A DAYLIGHT REDIRECTING COMPONENT

L. O. Grobe[1,2]; A. Noback[1]; S. Wittkopf[1]; Z. T. Kazanasmaz[2]

[1] *Lucerne University of Applied Sciences and Arts, Technikumstrasse 21, CH-6048 Horw*
[2] *Izmir Institute of Technology, Department of Architecture, Urla, TR-35430 Izmir*

## ABSTRACT

The Bidirectional Scatter Distribution Function (BSDF) of a selected Daylight Redirecting Component (DRC) is computed by a virtual goniophotometer using the enhanced photon map extension in Radiance, and compared to measured BSDF data.

The DRC comprises a stack of tilted aluminum louvers with configurable inclination angle. The profile of the louvers is designed to control transmission depending on sun altitude, and to redirect light up towards the ceiling.

The measured BSDF of the DRC is obtained from a scanning goniophotometer. For a sparse set of three source directions, the distribution is recorded at $\simeq$ 250,000 receiver directions. The asymmetric angular resolution allows detailed observation of characteristic features in the distribution, which are assumed to persist over a range of source directions. For each pair of source and receiver directions in the measurement, the computed BSDF is generated from a model of the DRC, replicating the measurement with a virtual goniophotometer. The simulation relies only on the enhanced photon map extension for Radiance. The BSDF from measurement and simulation are compared qualitatively and quantitatively to discuss the degree of accordance. The presence of characteristic features and their topology is evaluated by comparing polar surface plots of the distributions and profiles of the scatter plane. The direct-hemispherical transmission is compared for each measurement and simulation. The RMSE of each computed distribution against the corresponding measurements is calculated to quantify the directionally resolved deviation.

A high degree of qualitative accordance between the computed and the measured BSDF is achieved. Prominent features in the BSDF are represented by the model. A deviation of $-6\%$ to $+15\%$ is observed in a quantitative comparison of direct-hemispherical transmission by integration of computed and measured BSDF. The RMSE indicates higher deviations for lower source altitudes, where a direct transmission peak in the distribution is underestimated by the model. The method is proposed as a means to validate the capability of the enhanced photon map to predict transmission through DRC.

*Keywords: daylight simulation, modeling, validation, daylight redirection, BSDF*

## INTRODUCTION

Daylight Redirecting Components (DRC) reduce solar gains and energy demands for electrical lighting in buildings, and improve visual comfort for occupants. Planners aim at finding the minimum required transmission providing sufficient and evenly distributed illuminance during occupancy hours. Daylight simulation supports this optimization by providing illuminance and luminance data for assessments based on metrics such as Spatial Daylight Autonomy and Daylight Glare Probability.

Light transport through DRC [1] is a challenge to backward ray-tracing algorithms such as implemented in Radiance [2]. To avoid the limitations of the stochastic indirect-diffuse algorithm, the transmission through DRC can be pre-computed by dedicated software [3]. The geometry of the DRC is then replaced by the corresponding average Bidirectional Scatter Distribution Function (BSDF) [4, 5] as a uniform property. In the direct calculation, the actual geometry can be maintained to preserve phenomena such as shadow patterns or the visibility of geometric detail.

While the abstraction of DRC by their BSDF has been demonstrated as a suitable method for the calculation of illuminance and derived metrics [6], detail in the patterns of highlights and shadows caused by non-uniform transmission is lost. Such phenomena influence the visual appearance of adjacent surfaces and may affect visual comfort and glare probability. The reuse of pre-computed BSDF as libraries can reduce the time-consuming computation of BSDF. However, when relying on pre-computed BSDF, the parameters determining the BSDF are not accessible during the simulation, hindering e.g. the application of optimization algorithms that need to vary such parameters based on the simulation outcomes. To consider e.g. the adaptivity of a louver system by changing tilt angles, for any possible configuration a pre-computed BSDF would have to be provided.

An enhanced implementation of a forward-tracing photon-mapping algorithm in Radiance addresses these limitations [7]. Combined with advanced techniques such as progressive photon-mapping, it has been demonstrated to be capable to maintain even subtle patterns of reflection, including concentration and redirection [8].

## METHOD

This work proposes that a model of a sample is valid, if the BSDF calculated from it matches the measured BSDF of the sample. For this to be true, the model must accurately represent the geometry and surface properties of the sample. The measurement conditions, such as the illuminator and the resolution, must be replicated in the simulation. If both conditions are met, the computed BSDF can be compared to the measurement.

The BSDF of a DRC sample (figure 2), consisting of 39 fixed slats, is measured using a scanning goniophotometer [9]. As the redirection properties of the DRC depend on the louver assembly, the glazing is not included. To cover a representative area by the measurement, the illuminator is configured to a sampling aperture [5] of diameter $d_i \simeq 65mm$ on the sample with a collimated beam. The sampling aperture covers 6-7 slats of the DRC. A short-pass filter blocks wavelengths in the near infrared and limits the measurement to visible light. During the measurement, the receiver records irradiance at regular time intervals in a continuous scanning movement around the center of the sample, at a distance of $d_s = 1020mm$. First, the receiver scans the unobstructed beam and records the irradiance received, $E_{s,n}$. The power in the unobstructed beam, equal to the incident power on the sample, $P_i$, is calculated from $n$ measurements of $E_{s,n}$ and their corresponding solid angles $\Omega_{s,n}$:

$$P_i = \sum_n E_{s,n}\Omega_{s,n} \tag{1}$$

After the measurement of the beam, the distributions of $E_{s,n}$ after transmission through the sample are scanned at high resolution for three source directions $\theta_i = 35°, 40°, 45°$ (with invariant $\phi_i = 0°$). The scan path is refined in areas where high variance of the signal is observed, leading to an adaptive resolution of the measurement. By dividing each

of the $n$ measurements by $P_i$, the Differential Scattering Function DSF and the BSDF can then be calculated for each combination of $(\theta_i, \phi_i)$ and $(\theta_s, \phi_s)$:

$$BSDF_n = \frac{DSF_n}{\cos\theta_{s,n}} = \frac{E_{s,n}}{P_i \cdot \cos\theta_{s,n}} \tag{2}$$

The division by $\cos\theta_s$ as defined in the BSDF formulation leads to anomalies at source directions $\theta_s \simeq 90.0°$. As can be seen in equation 2, describing the transmission characteristics by the DSF is equivalent to the BSDF [5]. For better comprehensiveness, the DSF formulation is used in the comparison and in the discussion of results.

Based on the slats' profiles, inclination angles and distances (figure 2), a geometric model of the sample is prepared. The reflection properties of the slats' surfaces are modeled using the metal and plastic materials in Radiance. A virtual goniophotometer is set up to compute the BSDF of the model. The illuminator comprises a distant source with an opening angle of $\alpha = 0.5°$, illuminating a sample aperture of $d_i = 70mm$ diameter resembling the collimated beam of the measurement. A spherical receiver surface to store photon hit points surrounds the sample and represents possible positions of the receiver. The setup of this virtual goniophotometer and the orientation of the sample coordinate system is shown in figure 1.

Each simulation consists of a photon-distribution and a photon-gathering pass. In the first pass, photons are distributed from the light source and stored in photon maps after hitting the sample or the receiver sphere. In the second pass, the indirect irradiance on the receiver surface is estimated from the (local) photon density (rtrace -ab -1) on the receiver surface. For each receiver position recorded in the measurement, the irradiance $E_{s,n}$ is computed.

First, the distribution of the unobstructed beam is scanned in analogy to the procedure of the physical goniophotometer. The integral of the resulting set of measurements is calculated as a measure of the power received by the sample $P_i$ as in the measurement.

With the simulation model of the sample placed in the center of the receiver sphere, the source is rotated to the source directions [5] ($\theta_i = 35°, \theta_i = 40°, \theta_i = 35°$, later on referred to as source altitude, in the scatter plane $\phi = 0°$). The irradiance distribution on the receiver surface is computed for the entire transmission hemisphere ($\theta_s = 90°$ to $\theta_s = 180°$, $\phi_s = 0°$ to $\phi_s = 360°$). The DSF for any receiver location is then defined by equation equation 2.

Polar plots of the measured and computed DSF, centered at $\theta = 180°, \phi = 0°$ with the radius corresponding to the altitude angle $\theta$, are provided. To enhance visibility of details, a logarithmic scale is applied to the z-axis. The occurrence, location and shape of features such as peaks, ridges and other structures that are observed in the computed DSF shall match those in the measurement.

For a quantitative comparison, the integral of the computed DSF for each source direction, the transmission $\tau$, is compared to the measured transmission. Root Mean Square Error RMSE and Coefficient of Variance CV are calculated for each source direction:

$$RMSE = \sqrt{\left\langle |DSF_{n,comp} - DSF_{n,meas}|^2 \right\rangle}, \qquad CV = \frac{RMSE \cdot 2}{|DSF_{n,comp}| + |DSF_{n,meas}|} \tag{3}$$

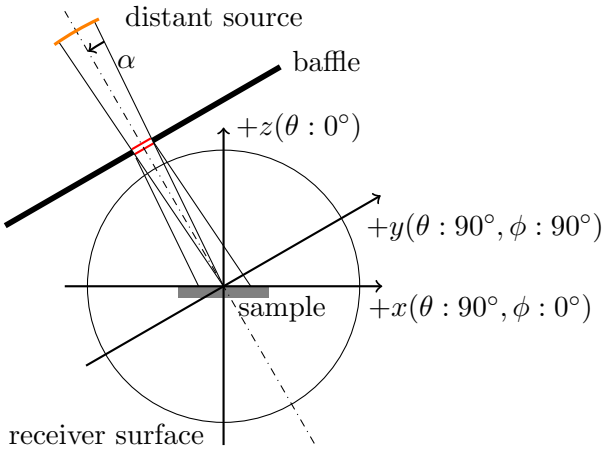


*Figure 1: Sample coordinate system and setup of the virtual goniophotometer used in the computation of the BSDF.*

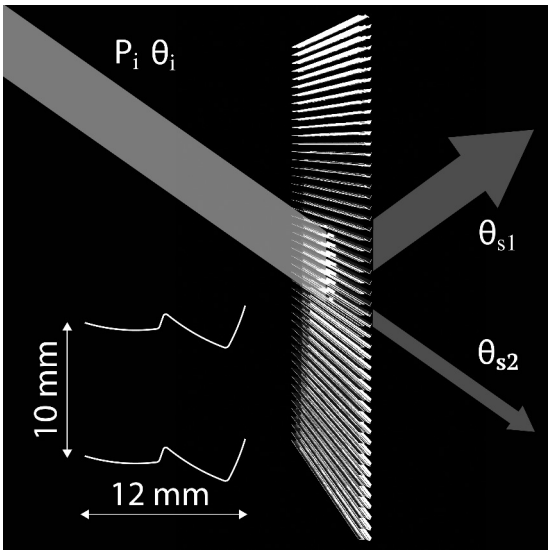


*Figure 2: Main transmission directions through the DRC (Luxtherm, patent Köster), profile of the slats.*

## RESULTS

The computed and measured DSF show the same topology of peaks and ridges (figures 3, 4). For both presented source directions, a ridge, ranging from $\theta = 130°$ to $\theta = 180°$, indicates upwards redirection by the reflector. The ridge is labeled as $\theta_{s,1}$ on the plots and corresponds to the range of upwards-scatter in figure 2. Both, the computed and the measured DSF, show a diffuse background with a characteristic trench due to the linear structure of the system. The computed transmission appears to be less smooth, spikes can be observed especially in the ridges.

At a source altitude of $\theta = 35°$ (figures 3, 4), a direct transmission peak (labeled $\theta_{s,2}$, as in figure 2) is visible at $\theta = -145°$ in the computed and measured distributions. Compared to the upwards-directed ridge $\theta_{s,1}$, the direct transmission peak is higher in the measured, lower in the computed distribution.

Direct transmission is blocked at a source altitude of $\theta = 45°$. A second, weaker ridge arises in a range from $\theta = -90°$ to $\theta = 180°$, indicating light transmitted downwards by reflection in the system. Redirection towards the ceiling ($\theta_{s,2}$) is maintained.

Directional-hemispherical transmittance [4] was calculated from the DSF for three source directions using equation 1 and is shown in table 1. A deviation in a range from -6% to +15% is observed. At a source altitude of $\theta = 35°$, with direct transmission occurring, the computed integral is lower than the measured one. Both RMSE and CV indicate a better fit for higher source altitudes, as can be seen in table 2.

| | $\theta_{in} = 35°$ | $\theta_{in} = 40°$ | $\theta_{in} = 45°$ |
|---|---|---|---|
| $\tau_m$ | 0.398 | 0.434 | 0.479 |
| $\tau_c$ | 0.376 | 0.493 | 0.549 |

*Table 1: Measured and computed direct-hemispherical transmission $\tau_m$, $\tau_c$.*

| | $\theta_{in} = 35°$ | $\theta_{in} = 40°$ | $\theta_{in} = 45°$ |
|---|---|---|---|
| *RMSE* | 0.1164 | 0.0283 | 0.0166 |
| *CV* | 0.6624 | 0.0615 | 0.0323 |

*Table 2: Root Mean Square Error RMSE and Coefficient of Variance CV.*

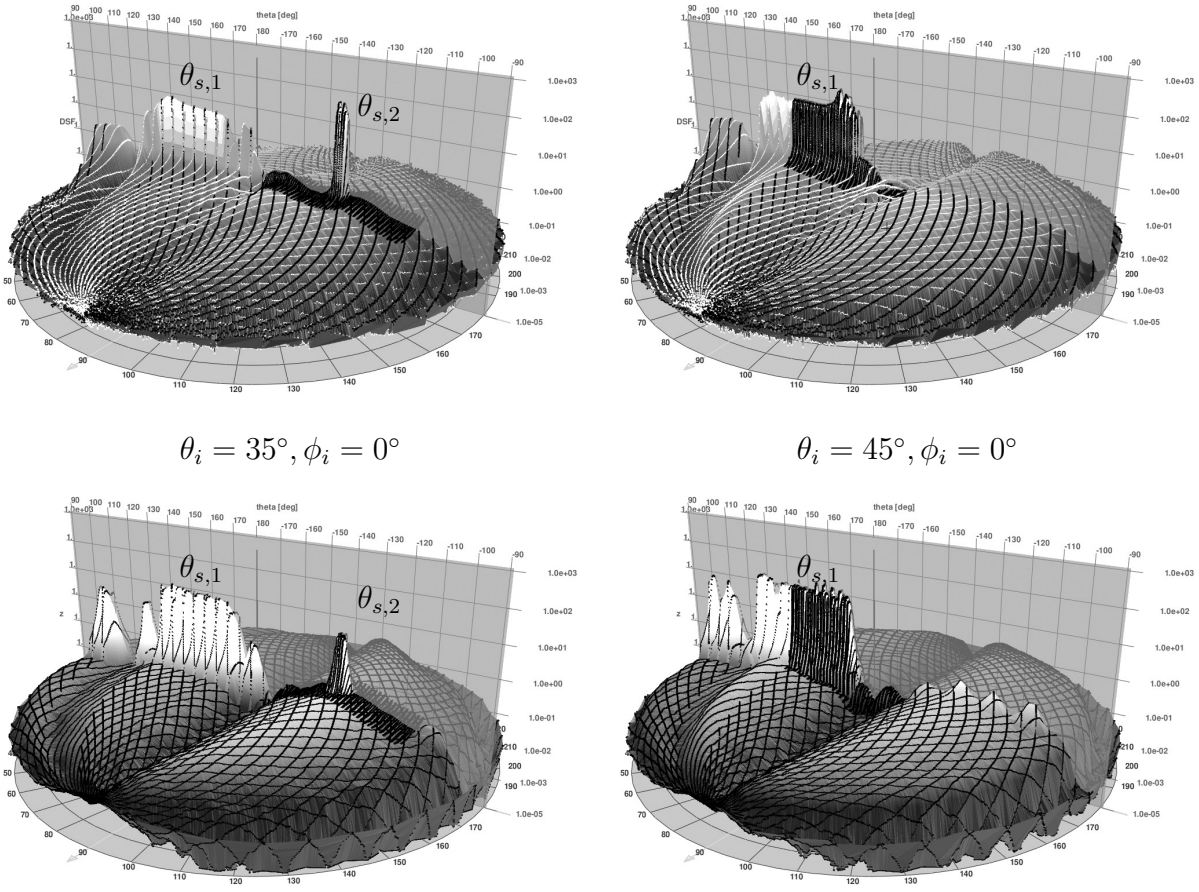


*Figure 3: Measured (top) and computed (bottom) DSF for two source altitudes. The dark lines indicate the path of the receiver in the measurement and the simulation.*

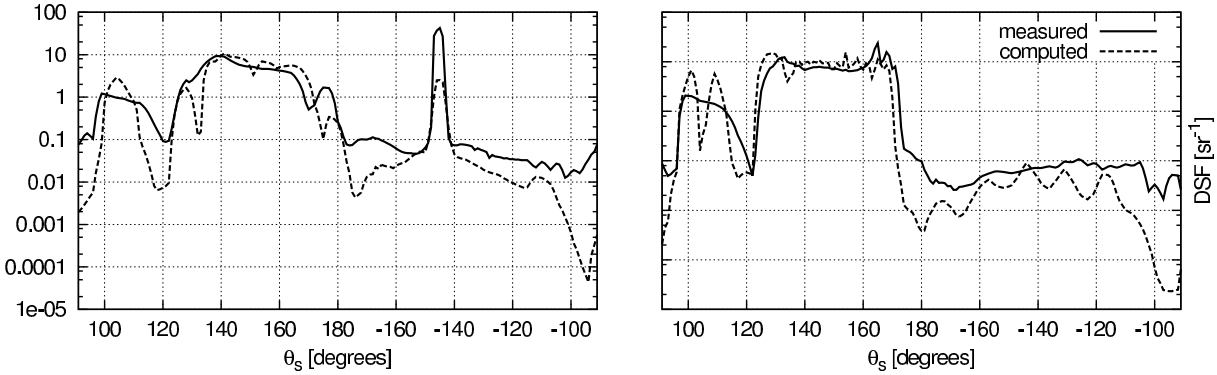


*Figure 4: Profiles of the measured and computed DSF in the scatter plane ($\phi = 0°$) for two source altitudes $\theta_i = 35°$ (left) and $\theta_i = 45°$ (right).*

## DISCUSSION

The comparison of computed and measured DSF has shown that, in principle, the enhanced photon map extension for Radiance is capable to model transmission through DRC and to represent the characteristic features in the distribution.

A better understanding of the observed deviations requires further investigation of the simulation algorithm and its parametrization, the measurement and the particular sample. Artifacts such as spikes in the DSF are expected for a faceted surface model, and can be controlled by its geometric resolution. The deviations in the computed and measured direct-hemispherical transmission, related to the underestimated direct transmission, require further investigation. Particular conditions of measurement and sample must be considered as well as the inherent bias [7] of the simulation algorithm. The selected DRC, with its angular selectivity and cut-off angles, is a particular challenge, as slight deviations between model and physical sample can cause drastic changes in the transmission. The measured BSDF as a reference is of limited reliability, as imperfections of the sample and the instrument signature have a high impact on both qualitative and quantitative results.

## ACKNOWLEDGMENTS

This research was supported by the Swiss National Science Foundation as part of the project Simulation- based assessment of daylight redirecting components for energy savings in office buildings (#147053). This contribution benefits from the doctoral degree support scheme of Lucerne University of Applied Sciences and Arts in collaboration with Izmir Institute of Technology. At the same time I would like to show my appreciation to my colleagues Marek Krehel for providing me with the measured BSDF data and Roland Schregle, author of the enhanced photon map extension for Radiance, for his support.

## REFERENCES

1. Köster, H.: Automatic heat control with mirror optics. In *Proceedings of the 3rd Workshop on Transparent Insolation*, 1989.
2. Larson, G. W., Shakespeare, R., Ehrlich, C., Mardaljevic, J., Phillips, E., and Apian-Bennewitz, P.: *Rendering with Radiance: the art and science of lighting visualization*. Morgan Kaufmann San Francisco, CA, 1998.
3. Kohler, C.: Simulation of complex glazing products; from optical data measurements to model based predictive controls. 2014.
4. Nicodemus, F. E., Richmond, J. C., Hsia, J. J., Ginsberg, I. W., and Limperis, T.: *Geometrical considerations and nomenclature for reflectance*, volume 160. US Department of Commerce, National Bureau of Standards Washington, DC, USA, 1977.
5. ASTM: Standard practice for goniometric optical scatter measurements. In *ASTM E 2387-05*. ASTM International, 2005.
6. McNeil, A., Jonsson, C., Appelfeld, D., Ward, G., and Lee, E.: A validation of a ray-tracing tool used to generate bi-directional scattering distribution functions for complex fenestration systems. *Solar Energy*, 98:404 – 414, 2013.
7. Schregle, R. Development and integration of the Radiance Photon Map Extension. Technical report, Lucerne University of Applied Sciences and Arts, 2015.
8. Schregle, R., Grobe, L., and Wittkopf, S.: Progressive photon mapping for daylight redirecting components. *Solar Energy*, 114:327–336, 2015.
9. Apian-Bennewitz, P.: New scanning gonio-photometer for extended BRTF measurements. In *SPIE Optical Engineering+ Applications*. SPIE, 2010.